

# Rheological Behavior of a Polymer Melt under the Impact of a Vibration Force Field

Guang-sheng Zeng, Jin-ping Qu

National Engineering Research Center of Novel Equipment for Polymer Processing, The Key Laboratory of Polymer Processing Engineering Ministry of Education, South China University of Technology, Guangzhou 510641, China

Received 22 November 2006; accepted 20 March 2007

DOI 10.1002/app.26562

Published online 8 July 2007 in Wiley InterScience (www.interscience.wiley.com).

**ABSTRACT:** A model for the molecular motion of a polymer melt under the impact of a vibration force field was developed. From complicated theory deduction, an expression of the relaxation time and dynamic apparent viscosity were obtained. The effect of a vibration frequency and amplitude on the melt's dynamic apparent viscosity is explained in terms of shear-thinning and untie-tangle crite-

ria. The model is supplemented by a calculation sample and experiment, which show that dynamic apparent viscosity of a melt will tend to decrease as the vibration frequency or amplitude increases. © 2007 Wiley Periodicals, Inc. *J Appl Polym Sci* 106: 1152–1159, 2007

**Key words:** melt; rheology; molecule; viscosity; polymer

## INTRODUCTION

Application of a vibration force field during polymer processing is a relatively new innovation and a valid processes method. There are two types of vibration force field that are used to modify the molding process and/or the properties of molded materials: One type is ultrasonic vibration and the other is mechanical shaking/oscillation. Lemelson<sup>1</sup> described an apparatus and method for controlling the internal structure of plastics in a mold by application of ultrasonic energy to the solidifying material to beneficially control the crystalline structure formed upon solidification. Pendleton<sup>2</sup> also describes an ultrasonic process to modify the structure of crystallizable thermoplastic materials. In one embodiment of Pendleton's invention, air-jet mono-whistles, consisting of a resonant chamber and an exponential horn, are directed at a tubular bubble being blown extruded as it passes the area above the annular orifice and below the frost line. The objective is to break down the large spherulites by ultrasonic energy to improve clarity of the blown films.

Schramm<sup>3</sup> demonstrated, as early as 1976, that vibrating the nozzles of injection molding machines resulted in higher throughputs and with parts

suffering less shrinkage. He attributed the absence of shrinkage to a delay in freezing at the gate caused by friction heating from the mechanical vibration, allowing the part to solidify under continuous pressure. In Allen and Bevis's<sup>4,5</sup> work, the polymer melt is split into two identical feeds. Each feed is equipped with its own packing chamber and piston, and is capable of supplying pressure to the cavity independently of the other. During the molding cycle, the molten polymer is injected from the barrel into the mold through one or both piston channels in the processing head, depending on the desired program. Once the mold is filled the pistons are actuated in a selected sequence. The piston action first develops fluctuating melt pressures that moves and shears the melt across the weld and across the weld line in the cavity and gate areas. This results in actually shaking the melt fronts to increase the interface area while eliminating trapped air between the two colliding fronts. This is caused by the actuation of the compression–decompression forces on the melt by the dual feed design. New material can be introduced to compensate for shrinkage and/or voids.

Using a vibration of a screw along its axis direction, Qu<sup>6</sup> produced mechanical vibration in a screw extruder for a polymer molding process, which includes a solid conveying, melting, melt conveying and molding segments. In his work, the screw can move back and forth under the impact of electromagnetic force or by pulsed hydraulic pressure. This device had a vibration frequency range 0–100 Hz, and an amplitude range 0–30 mm. The result of Qu's work<sup>7–11</sup> indicates that the vibration force field can compact the material feed either in form of granules or powders, generate viscous dissipation heat, even out the heat

Correspondence to: J.-p. Qu (jpqu@scut.edu.cn).

Contract grant sponsor: National Natural Science Foundation of China; contract grant numbers: 20074010, 10472034, 10590351.

Contract grant sponsor: Doctorate Foundation of South China University of Technology.

*Journal of Applied Polymer Science*, Vol. 106, 1152–1159 (2007)  
© 2007 Wiley Periodicals, Inc.

distribution, increase the throughput, avoid trapping of bubbles between the granules, and create orientation effects of polymer molecules in the melt which thereby obtain a more homogeneous product with better mechanical properties.

Many researchers indicate that material rheology is a function of vibration frequency and amplitude in addition to temperature and pressure. This can be put to practical use to influence diffusion- and rate-sensitive processes which depend on viscosity and relaxation kinetics, such as nucleation and growth of crystals, blending, and orientation. Nevertheless, until now, no publication about polymer molecular motion under the impact of a vibration force field can be found. The aim of this work is to determine the effect of a vibration force field on the molecular motion in polymer melts. To do this, both experimental and modeling studies have been performed.

### MODEL DEVELOPMENT

Because of its long molecular chain and high molecular weight, a polymer melt behaves as a strong non-linear viscoelastic material. Long molecular chains and chain segments of polymer melt continue moving and never stop. The interactions between molecules or molecular segments are very complicated. Thereby, to reduce the intricacies of the many-body system, a model of linear polymer chains is established (see Fig. 1). In this model, one single linear polymer chain is simplified as a bead with a rubber band. The elastic action from another molecule chain is denoted by the elastic band, and the viscous action caused by surrounding chains is translated into the frictional force on the bead. Then the molecules in a cubed unit can be represented as  $N$  beads connected by rubber bands of root-mean-square size  $b$ , as shown in Figure 1. The beads in this model only interact with each other through the connecting rubber bands. Each bead is characterized by its own independent friction with the friction coefficient  $\zeta$ .

Consider only the vibration response in  $x$  direction of this system; the effects of the vibration force field on the molecules along various directions are not the same. A molecule that is parallel to the vibration direction suffers the most impact, while there is little if any effect on a molecule that is perpendicular to the vibration direction, and the effects on the molecules

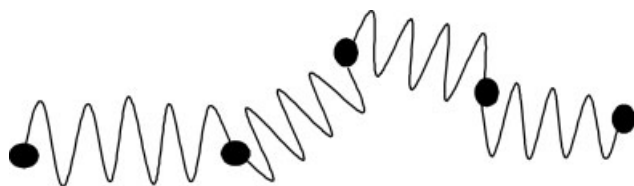


Figure 1 Three-dimensional model of molecular chains.



Figure 2 One-dimensional model of molecular chains.

along other directions are between the former and the latter. Since that the macromolecule is assumed to be linear, and the vibration is along a single direction, this problem can be linearized. That is, the macromolecule in three-dimensional space can be projected onto a one coordinate axis (herein it is  $x$ ), and the mean-square end-to-end distance of each molecule is also projected on to the axis; then by using the “validity-elasticity-constant” which is in  $x$  direction, the linear macromolecule can be simplified as a one-dimension bead-rubber-band chain (shown in Fig. 2).

As stated above, this work focuses on the polymer melt. Stress in solids are proportional to deformation (for small deformations), but the stress in liquids depends only on the rate of deformation, not the total amount of deformation. If a sphere of radius  $R$  moves in a liquid of viscosity  $\eta$ , a simple dimensional argument can determine the friction coefficient of the sphere. The friction should depend only on the viscosity of the surrounding liquid and the sphere size:

$$\zeta(\eta, R) \quad (1)$$

The coefficient of friction is the ratio of force-velocity ( $\text{kg s}^{-1}$ ). The viscosity is the ratio of stress-shear rate ( $\text{kg m}^{-1} \text{s}^{-1}$ ) and the sphere radius (m). The only functional form that is dimensionally correct gives a very simple relation:

$$\zeta = \eta R \quad (2)$$

The full calculation of the slow flow of liquid past a sphere was published by Stokes in 1880, yielding the numerical prefactor of  $6\pi$  that results in Stokes law:

$$\zeta = 6\pi\eta R \quad (3)$$

If we suppose

$$R = l/2 \quad (4)$$

Then we have

$$\zeta = 3\pi\eta l \quad (5)$$

where  $l$  is the length of the molecular chain. Then the total friction coefficient of the whole bead-band chain is the sum of the contributions of each of the  $N$  beads:

$$\zeta_N = N\zeta = 3\pi N\eta l \quad (6)$$

The viscous frictional force the chain experiences if it is pulled with velocity  $\vec{v}$  is

$$\vec{f} = -\zeta_N \vec{v} = -3\pi\eta Nl\vec{v} \tag{7}$$

Moreover, many studies indicate that a materials rheology is a function of vibration frequency and amplitude in addition to temperature and pressure; that is, the application of a vibrational force field can affect viscosity  $\eta$ . Therefore,  $\eta$  should be modified before the following deduction. Assuming that the vibration equation in  $x$  direction is

$$\xi = A \sin(\omega t) \tag{8}$$

where  $A$  is the amplitude,  $\omega$  is the frequency. Thereby, from Refs. 8–11, we can let

$$\eta = K'\beta_0 \left\{ \frac{4n}{[3n + 1 + nM_B\eta_0 \frac{\omega}{a} \cos \phi_1]} \right\}^n \times \left[ b_1 + b_2 \exp\left(-b_3 \frac{R^3}{R_0^3} \bar{\dot{\gamma}}_a\right) \right] \tag{9}$$

where  $n$  is the power-law index,  $\beta_0$  is the modifying coefficient,  $K'$  is the consistency coefficient of Newtonian fluid,  $M_B$  is the geometry parameter of capillary rheometer,  $\eta_0$  is the zero shear apparent viscosity,  $b_1, b_2, b_3$ , and  $a$  are constants determined from experiment,  $R_0$  is the radius of capillary,  $\bar{\dot{\gamma}}_a = A\omega/\delta$  is the breadth of nominal shear rate,  $\phi_1$  is the phase angle.

Because of the vibration force field, each bead will deviate from its equilibrium position. Bead  $i$ 's, deviation is  $x_i$ ; moreover, considering the restoring force

generated by the rubber band and the friction from other medium, the equations are transformed as follows:

The friction force

$$\begin{cases} F_{x0} = -3\pi\eta Nl_0(\dot{x}_0 - \dot{x}_1), & i = 0 \\ \vdots \\ F_{xi} = -3\pi\eta Nl_i(-\dot{x}_{i-1} + 2\dot{x}_i - \dot{x}_{i+1}), & 1 \leq i \leq z - 1 \\ \vdots \\ F_{xz} = -3\pi\eta Nl_z(\dot{x}_z - \dot{x}_{z-1}), & i = z \end{cases} \tag{10}$$

To simplify the deduction, we can let

$$l_0 = l_1 = \dots = l_z = b \tag{11}$$

The deformation restoring force

$$\begin{cases} f_{x0} = -\frac{3kT}{b^2}(x_0 - x_1), & i = 0 \\ \vdots \\ f_{xi} = -\frac{3kT}{b^2}(-x_{i-1} + 2x_i - x_{i+1}), & 1 \leq i \leq z - 1 \\ \vdots \\ f_{xz} = -\frac{3kT}{b^2}(-x_{z-1} + x_z), & i = z \end{cases} \tag{12}$$

where  $k$  is the Boltzmann constant,  $T$  is the temperature.

Considering the inertial force of bead  $i$ :

$$F_{ia} = M \frac{d^2x_i}{dt^2} = M\ddot{x}_i \tag{13}$$

where  $M$  is the average molecular weight.

Therefore, from the balance of force we obtain

$$\begin{cases} 3\pi\eta Nb(\dot{x}_0 - \dot{x}_1) - M\ddot{x}_0 + \frac{3kT}{b^2}(x_0 - x_1) = 0, & i = 0 \\ 3\pi\eta Nb(-\dot{x}_{i-1} + 2\dot{x}_i - \dot{x}_{i+1}) - M\ddot{x}_i + \frac{3kT}{b^2}(-x_{i-1} + 2x_i - x_{i+1}) = 0, & 1 \leq i \leq z - 1 \\ 3\pi\eta Nb(-\dot{x}_{z-1} + \dot{x}_z) - M\ddot{x}_z + \frac{3kT}{b^2}(-x_{z-1} + x_z) = 0, & i = z \end{cases} \tag{14}$$

In the present model, molecules of polymer melt are driven by an oscillator. Each bead has a certain displacement, speed, and acceleration at a certain time  $t$ , and the acceleration is only relevant to

frequency; hence, we have

$$\ddot{x} = -\omega^2 x \tag{15}$$

Substituting eq. (15) into eq. (14) yields

$$\begin{cases} 3\pi\eta Nb(\dot{x}_0 - \dot{x}_1) + M\omega^2 x_0 + \frac{3kT}{b^2}(x_0 - x_1) = 0 & i = 0 \\ 3\pi\eta Nb(-\dot{x}_{i-1} + 2\dot{x}_i - \dot{x}_{i+1}) + M\omega^2 x_i + \frac{3kT}{b^2}(-x_{i-1} + 2x_i - x_{i+1}) = 0 & 1 \leq i \leq z - 1 \\ 3\pi\eta Nb(-\dot{x}_{z-1} + \dot{x}_z) + M\omega^2 x_z + \frac{3kT}{b^2}(-x_{z-1} + x_z) = 0 & i = z \end{cases} \tag{16}$$

or

$$C\dot{X} + DX + BCX = 0 \tag{17}$$

where

$$\dot{X} = \begin{bmatrix} \dot{x}_0 \\ \dot{x}_1 \\ \vdots \\ \dot{x}_z \end{bmatrix}, \quad D = \frac{M\omega^2}{3\pi\eta Nb} \quad (18)$$

$$B = \frac{kT}{\pi\eta Nb^3}, \quad X = \begin{bmatrix} x_0 \\ x_1 \\ \vdots \\ x_z \end{bmatrix} \quad (19)$$

$$C = \begin{bmatrix} 1 & -1 & 0 & 0 & \cdots & 0 & 0 \\ -1 & 2 & -1 & 0 & \cdots & 0 & 0 \\ \vdots & \vdots & \vdots & \vdots & \vdots & \vdots & \vdots \\ 0 & 0 & 0 & \cdots & -1 & 2 & -1 \\ 0 & 0 & 0 & \cdots & 0 & -1 & 1 \end{bmatrix}_{(Z+1) \times (Z+1)} \quad (20)$$

**RELAXATION TIME**

Before solving eq. (17), we can let:

$$C = L^T L, \quad C_R = L L^T \quad (21)$$

where

$$L = \begin{bmatrix} 1 & -1 & 0 & 0 & \cdots & 0 & 0 \\ 0 & 1 & -1 & 0 & \cdots & 0 & 0 \\ \vdots & \vdots & \vdots & \vdots & \vdots & \vdots & \vdots \\ 0 & 0 & 0 & \cdots & 0 & 1 & -1 \\ 0 & 0 & 0 & \cdots & 0 & 0 & 0 \end{bmatrix}_{(Z+1) \times (Z+1)} \quad (22)$$

$$L^T = \begin{bmatrix} 1 & 0 & 0 & 0 & \cdots & 0 & 0 \\ -1 & 1 & 0 & 0 & \cdots & 0 & 0 \\ \vdots & \vdots & \vdots & \vdots & \cdots & \vdots & \vdots \\ 0 & 0 & 0 & \cdots & -1 & 1 & 0 \\ 0 & 0 & 0 & \cdots & 0 & -1 & 0 \end{bmatrix}_{(Z+1) \times (Z+1)} \quad (23)$$

$$C_R = \begin{bmatrix} 2 & -1 & 0 & 0 & \cdots & 0 & 0 \\ -1 & 2 & -1 & 0 & \cdots & 0 & 0 \\ \vdots & \vdots & \vdots & \vdots & \cdots & \vdots & \vdots \\ 0 & 0 & 0 & \cdots & -1 & 2 & -1 \\ 0 & 0 & 0 & \cdots & 0 & -1 & 2 \end{bmatrix}_{(Z+1) \times (Z+1)} \quad (24)$$

Substituting eq. (21) into eq. (17) gives

$$LL^T L \dot{X} + LDX + BLL^T LX = 0 \\ \Rightarrow C_R L \dot{X} + LDX + BC_R LX = 0$$

Using coordinate transforming we have

$$Q^{-1} C_R Q = \Lambda = \{\lambda_p \delta_{pq}\} \quad (1 \leq p, q \leq z) \quad (26)$$

where

$$\delta_{pq} = \begin{cases} 0, & p \neq q \\ 1, & p = q \end{cases} \quad (27)$$

$$Q^{-1} Q = I \quad (28)$$

Q is the replacement matrix, I is the element matrix, Λ is the diagonal matrix. Then

$$C_R Q = Q \Lambda \quad (29)$$

Hence the following equation is obtained:

$$\begin{cases} (2 - \lambda_1) Q_{1,1} - Q_{1,2} = 0 \\ -Q_{2,1} + (2 - \lambda_2) Q_{2,2} - Q_{2,3} = 0 \\ -Q_{3,2} + (2 - \lambda_3) Q_{3,3} - Q_{3,4} = 0 \\ \vdots \\ -Q_{(z+1),z} + (2 - \lambda_z) Q_{(z+1),(z+1)} = 0 \end{cases} \quad (30)$$

Solving eq. (30) we have

$$\lambda_p = 2 - 2 \cosh[ip\pi/(z + 2)] = 4 \sin^2 \left[ \frac{p\pi}{2(z + 2)} \right], \\ p = 1, 2, 3, \dots, z + 1 \quad (31)$$

Then eq. (25) can be changed as

$$\Lambda Q^{-1} L \dot{X} - D Q^{-1} L X - B \Lambda Q^{-1} L X = 0 \quad (32)$$

Solving eq. (32) we have

$$X_p = c_1 \exp \left[ - \left( \frac{M\omega^2}{3\pi\eta Nb \lambda_p} + \frac{3kT}{a^2 3\pi\eta Nb} \right) t \right] \quad (33)$$

Moreover, from constrain vibration equation

$$\ddot{x} + 2\beta\dot{x} + \omega_0 x = A_0 \omega^2 \cos \omega t \quad (34)$$

where  $\beta = \frac{\gamma}{2M}$ , γ is the damping coefficient, β is the damp factor, ω<sub>0</sub> is the inherent frequency, here we can let

$$\omega_0 = \frac{3kT}{Mb^2} \quad (35)$$

Solving eq. (34) we have

$$x = A_0 \exp(-\beta t) \cos(\omega_0 t + \alpha) + A \cos(\omega t + \varphi) \quad (36)$$

where

$$A = \frac{A_0 \omega^2}{\sqrt{(\omega_0^2 - \omega^2)^2 + 4\beta^2 \omega^2}} \quad (37)$$

$$\tan \varphi = \frac{-2\beta\omega}{\omega_0^2 - \omega^2} \quad (38)$$

Then solving eq. (33) and eq. (36) we have

$$\begin{aligned} & \lim_{t \rightarrow 0} [A_0 \exp(-\beta t) \cos(\omega_0 t + \alpha) + A \cos(\omega t + \varphi)] \\ &= \lim_{t \rightarrow 0} \left\{ c_1 \exp \left[ - \left( \frac{M\omega^2}{\lambda_p} + \frac{3kT}{b^2} \right) \frac{t}{3\pi\eta N b} \right] \right\} \end{aligned} \quad (39)$$

Hence

$$c_1 = A_0 + A \cos(\varphi) \quad (40)$$

$$X_p = (A_0 + A \cos \varphi) \exp \left[ - \left( \frac{M\omega^2}{3\pi\eta N b \lambda_p} + \frac{3kT}{3\pi\eta N b^3} \right) t \right] \quad (41)$$

Thereby the relaxation time is obtained:

$$\tau_p = \frac{3\pi\eta N \lambda_p b^3}{M\omega^2 b^2 + 3kT\lambda_p} \quad (42)$$

### APPARENT VISCOSITY

From Maxwell–Weichert<sup>12–15</sup> model we have

$$\eta = \sum_{p=1}^z G_p \tau_p, \quad G_p = \frac{E_p}{3} \quad (43)$$

Then from rubber-elasticity theory and affine-distortion theory,<sup>12–15</sup> the apparent viscosity of polymer melt under the impact of vibration force field is obtained:

$$\eta = NkT \sum_{p=1}^N \frac{3\pi\eta N b \lambda_p a^2}{M\omega^2 a^2 + 3kT\lambda_p} \quad (44)$$

### EXPERIMENT

#### Apparatus

Apparatus for the present experiment is made in the National Engineering Research Center of Novel Equipment for Polymer Processing, South China University of Technology, China. Figure 3 shows the dynamic rheometer setup. As shown in Figure 3, the

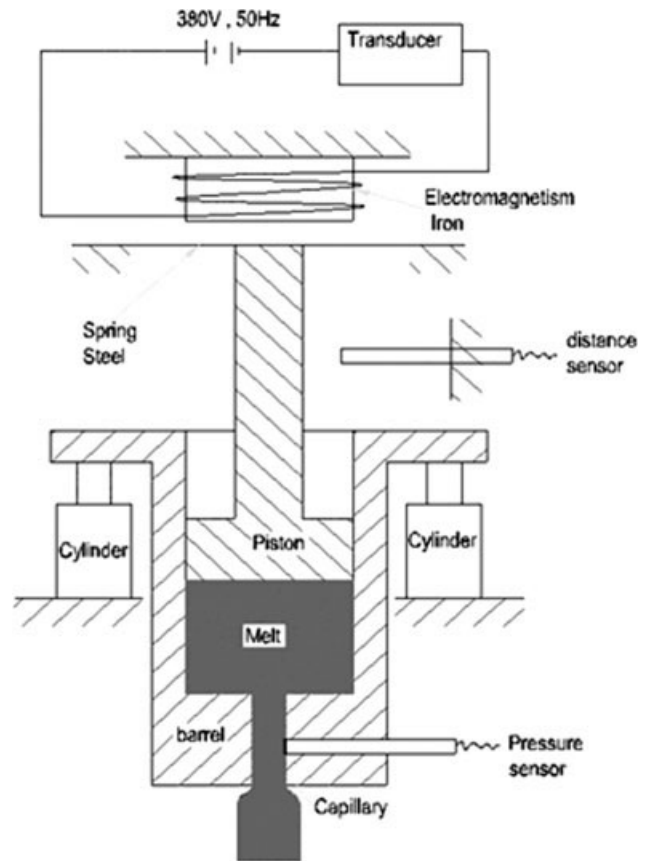


Figure 3 Illustration of the dynamic rheometer.

piston can vibrate up and down driven by the steel spring and the electromagnet. The transducer can adjust the vibration frequency and amplitude. The length-to-diameter ratio ( $L/D$ ) of the capillary is 40. The barrel can be pushed by the cylinder. The pressure sensor can capture the pressure data of the melt, and the distance sensor can determine the vibration frequency and amplitude promptly. The equipment can realize a frequency range of 0–50 Hz, and an amplitude range of 0–12 mm. The apparent viscosity is calculated using a computer with self-made software program.

#### Material properties

- High-density polythene (HDPE), made in Yangzhi Petrochemical Ltd., China, the type number is 5000 s,  $\rho = 0.95 \text{ g/cm}^3$ ,  $\bar{M}_w = 1.69 \times 10^5 \text{ g/mol}$ ,  $\eta_0 \approx 10^3 \text{ Pa s}$ , temperature for experiment is  $T = 473 \text{ K}$ , so  $N = 2.29 \times 10^{24}/\text{m}^3$ , for the chemical bond of the molecule of HDPE is C—C, and the length of C—C is  $1.54 \times 10^{-10} \text{ m}$ , therefore, we can obtain  $b^2 = 8.1 \times 10^{-16} \text{ m}^2$ , moreover, the Boltzman constant is  $k = 1.38 \times 10^{-23} \text{ J/K}$ .

- b. Low-density polythene (LDPE), made in Guangdong Maoming Petrochemical Ltd. China, the type number is 951-050,  $\rho = 0.920 \text{ g/cm}^3$ ,  $\bar{M}_w = 1.5 \times 10^5 \text{ g/mol}$ ,  $\eta_0 \approx 3 \times 10^3 \text{ Pa s}$ , temperature for the present experiment is  $T = 453 \text{ K}$ .
- c. Polypropylene (PP), made in Fenghuang Petrochemical Ltd., China, the type number is T30S,  $\rho = 0.89 \text{ g/cm}^3$ ,  $\bar{M}_w = 1.35 \times 10^5 \text{ g/mol}$ ,  $\eta_0 \approx 1.1 \times 10^2 \text{ Pa s}$ ,  $T = 483 \text{ K}$ .

Furthermore, from previous experiment we obtain:  $M_B = 1.517 \times 10^6/\text{m}$ ,  $n = 0.41$ ,  $K' = 1.45 \times 10^4 \text{ N s}^n/\text{m}^2$ ,  $a = 1.29 \times 10^{10} \text{ Pa/m}$ ,  $\beta_0 = 1$ ,  $b_1 = 0.724$ ,  $b_3 = 0.128 \times 10^3 \text{ s/m}$ ,  $R = 1.5 \text{ mm}$ ,  $R_0 = 4 \text{ mm}$ .

### Procedure

Load the polymer pellets (HDPE, LDPE, and PP respectively) into the barrel, and then set the temperature of the barrel to the desired value (HDPE is

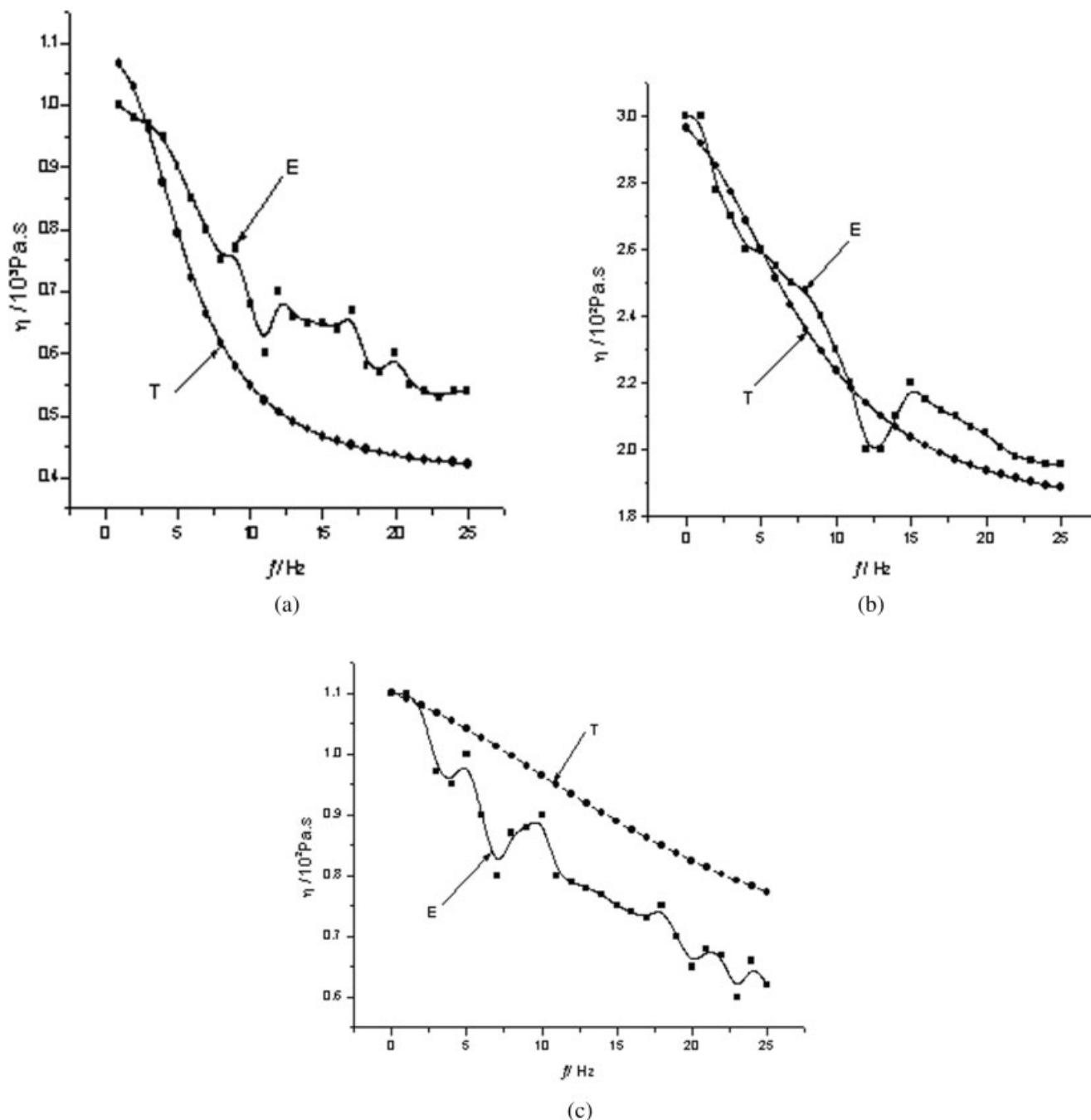


**Figure 4** Relationship between dynamic apparent viscosity and vibration frequency at  $A = 0.1 \text{ mm}$  (T—theoretical results, E—experimental results): (a) HDPE, (b) LDPE, and (c) PP.

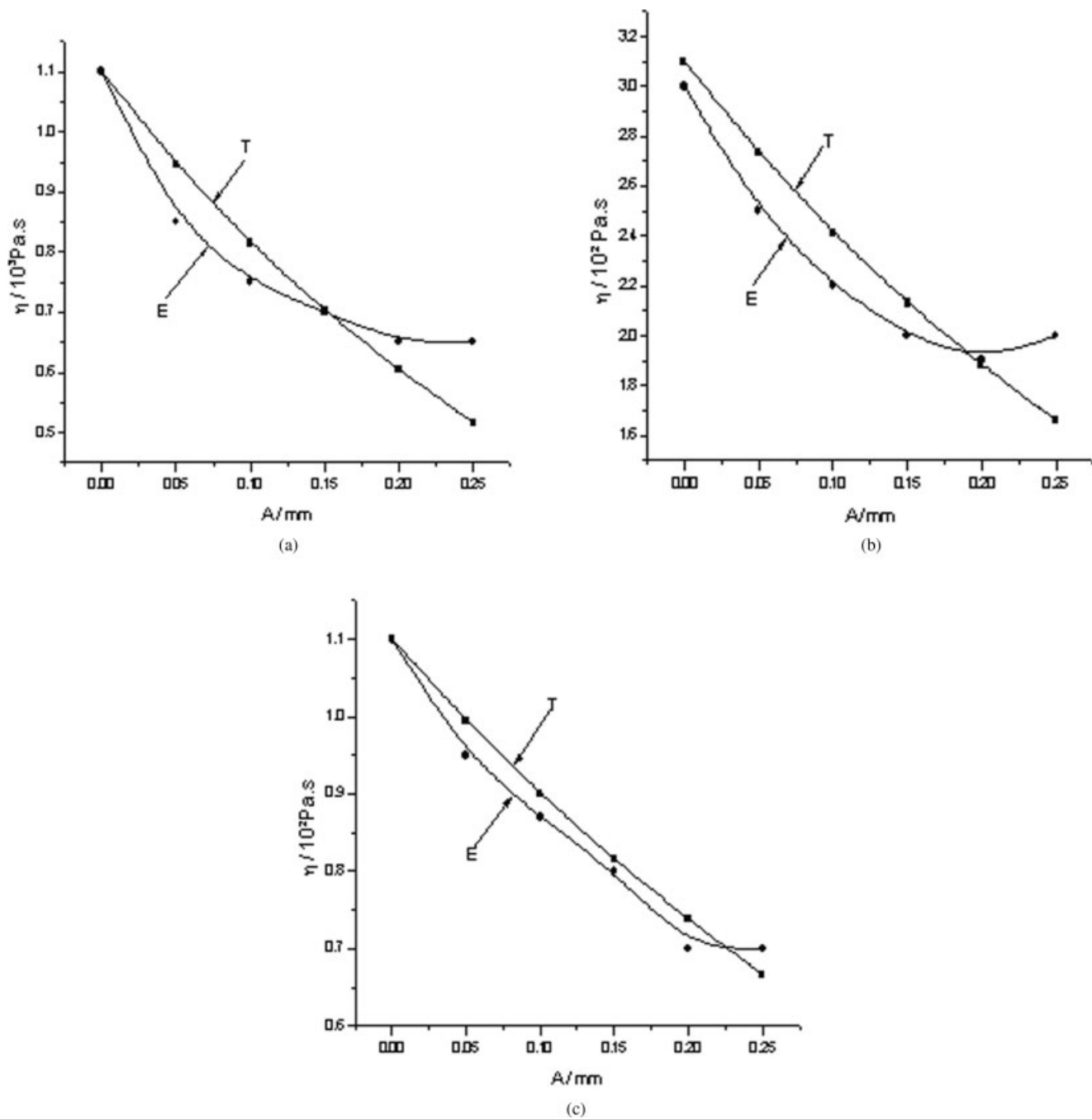


**Figure 5** Relationship between the dynamic apparent viscosity and the amplitude (T—theoretical results, E—experiment results): (a) HDPE, (b) LDPE, and (c) PP.

200°C, LDPE is 180°C, and PP is 210°C respectively); after the material is entirely melted, the electromagnet and the cylinder start to apply pressure. The moving speed of the cylinder is controlled at  $10^{-2}$  cm/s. The vibration amplitudes of the piston for the present experiment are 0, 0.05, 0.1, 0.15, 0.2, and 0.25 mm respectively. And the frequency can be adjusted from 0 to 20 Hz (in 1 Hz increments). The computer simultaneously, records the data for each vibration frequency and amplitude, and finally, plots the curve

that expresses the relationship between the dynamic apparent viscosity and the vibration frequency and amplitude.

## RESULTS AND DISCUSSION

Figure 4(a–c) are the relationships between the dynamic apparent viscosity and the frequency of HDPE, LDPE, and PP material respectively. The

application of vibration force field to a melt can orient molecules, untangle molecules and decrease internal friction. It is clear from Figure 4 that the dynamic apparent viscosity decreases as the frequency increases. But when the frequency is high enough, the dynamic apparent viscosity will arrive at a steady value. Further studying Figure 4 reveals that although the results of experiment are in good agreement with that of the calculation, there still some deviation between the experiment values and the calculation results. This is because the present model is based on the long linear molecule chain, but in fact, most of the polymer molecules have branched chains, and some are even cyclic. The interaction between branched chains, rings, and linear chains will block the free flowing of the polymer macromolecule, and thus increase the apparent viscosity of polymer melt.

Figure 5(a–c) shows the relationship between dynamic apparent viscosity and vibration amplitude of HDPE, LDPE, and PP respectively. As shown in Figure 5, the dynamic apparent viscosity decreases as the amplitude increases, where T denotes the theoretical curve and E denotes the experimental data. Notice in Figure 5(a), that the dynamic apparent viscosity of HDPE coming from experimental data decrease from about 1100 to about 680 Pa s in traversing from  $A = 0$  to  $A = 0.25$  mm (a about 38.2% decrease). Similarly, the dynamic apparent viscosity of LDPE coming from experiment decrease from about 300 to about 200 Pa s, going from  $A = 0$  to  $A = 0.25$  mm (a about 30% decrease), and the dynamic apparent viscosity of PP of the experiment result in Figure 5(c) is found to be decreased from about 110 to about 70 Pa s, going from  $A = 0$  to  $A = 0.25$  mm. Combining all of the aforementioned data, it appears that the introduction of vibration force field can decrease the dynamic apparent viscosity to great degree. Inspecting the curves plotted in Figure 5 reveals that when the vibration amplitude approaches an extremum, continuing to increase vibration amplitude will not lead to a significant change of the dynamic apparent viscosity, since it had already reached a relative steady value. As seen in Figure 5, although the results of experiment are very consistent with our theoretical calculation, there

are still minor deviations among them. This is because, many assumptions were made during the theory deduction to obtain the analytical expressions of the apparent viscosity, which were not neglected in the real world. On the other hand, test error is another reason for the deviation.

## CONCLUSIONS

Bead–rubber-band model has been established which can depict the motion of polymer molecule under the impact of vibration force field. Relation expressions of the relaxation time and the dynamic apparent viscosity have been obtained. The results from the calculation sample and the experiment indicated that, the dynamic apparent viscosity of a melt will decrease as the vibration frequency and amplitude increase, but when the frequency or the amplitude is high enough, further increases will not affect the dynamic apparent viscosity. The comparison of the results of the experiment and the calculation sample prove that the present theory is valid, efficient and useable.

This study will serve as the theoretical basis for the optimum conditions of polymer material processing and novel equipment design.

## References

1. Lemelson, J. U.S. Pat. 4,288,398 (1981).
2. Pendleton, J. W. U.S. Pat. 3,298,065 (1965).
3. Schramm, K. W. Doctor-Engineer Thesis, Rhenish-Westphalian College of Technology, 1976.
4. Allen, P. S.; Bevis, M. U.S. Pat. 4,925,161 (1985).
5. Ibar, J. P. *Polym Eng Sci* 1998, 38, 1.
6. Qu, J.-p. U.S. Pat. 5,217,302 (1993).
7. Qu, J.-p. *J South China Univ Technol (Natural science)* 1992, 20, 1.
8. Qu, J.-p.; Zeng, G.-s. *J Chem Indust Eng (China)* 2006, 57, 414.
9. Zeng, G.-s.; Qu, J.-p. *J Chem Indust Eng (China)* 2006, 57, 424.
10. Zeng, G.-s.; Qu, J.-p. *Chin J Mater Res* 2006, 20, 59.
11. Qu, J.-p.; Zeng, G.-s. *J Appl Polym Sci* 2006, 100, 3860.
12. Kirkwood, J. G. *Rec Trav Chim Pays-Bas* 1949, 68, 649.
13. Rouse, P. E., Jr. *J Chem Phys* 1953, 21, 1271.
14. De Gennes, P. G. *J Chem Phys* 1971, 55, 572.
15. Doi, M.; Edwards, S. F. *J Chem Soc Faraday Trans* 1978, 2, 1702.